

In the systems of all dimensions we studied here, it fluctuates around a zero average with a mean square value which scales with the height of the main resonance peak, G_F and is inversely proportional to the conductance $g(L_F)$ (measured in quantum units) of a piece of disordered electrode with typical dimensions $L_F \sim \sqrt{\hbar D/\Gamma}$ determined by the width of the resonance itself:

$$\left\langle \left(\frac{dI}{dV} \right)^2 \right\rangle \sim \frac{G_F^2}{g(L_F)}.$$

The value of the correlation magnetic field of fluctuations is also related to the length L_F , $\Delta B_c \sim \phi_0/L_F^2$ and the correlation properties of the pattern of dI/dV with respect to the voltage variations are found in an analytical form both in two and three dimensions as a function of the voltage scaled by the width of the main resonance peak. Both the amplitude of fluctuations and the correlation parameter ΔB_c are expected to increase with the magnetic field.

The author thanks EPSRC for support.

References

1. Lerner I V *Phys. Lett. A* **133** 253 (1988)
2. Al'tshuler B L, Shklovskii B I *Zh. Eksp. Teor. Fiz.* **91** 220 (1986) [*Sov. Phys. JETP* **64** 127 (1986)]
3. Altshuler B, Kravtsov V, Lerner I, in *Mesoscopic Phenomena in Solids* (Modern Problems in Condensed Matter Sciences Vol. 30, Eds B L Altshuler, P A Lee, R A Webb) (Amsterdam: North-Holland, 1991)
4. Wegner F Z. *Phys. B* **36** 209 (1980); Fal'ko V I, Efetov K B *Europhys. Lett.* **32** 627 (1995); *Phys. Rev. B* **52** 17413 (1995)
5. Fal'ko V I, Efetov K B *J. Math. Phys.* **37** 4935 (1996)
6. Efetov K B *Adv. Phys.* **32** 53 (1983)
7. Nazarov Yu V *Zh. Eksp. Teor. Fiz.* **98** 306 (1990) [*Sov. Phys. JETP* **71** 171 (1990)]; Zyuzin A Yu, Spivak B Z *Zh. Eksp. Teor. Fiz.* **98** 1011 (1990) [*Sov. Phys. JETP* **71** 563 (1990)]
8. Lerner I V, Raikh M E *Phys. Rev. B* **45** 14036 (1992)
9. Su B, Goldman V J, Cunningham J E *Science* **255** 313 (1992); *Phys. Rev. B* **46** 7644 (1992)
10. Dellow M W et al. *Phys. Rev. Lett.* **68** 1754 (1992); Geim A K et al. *Phys. Rev. Lett.* **72** 2061 (1994); McDonnell P J et al. *Physica B* **211** 433 (1995)
11. Tewordt M et al. *Phys. Rev. B* **46** 3948 (1992); *Phys. Rev. B* **45** 14407 (1992); Schmidt T et al. *Phys. Rev. B* **51** 5570 (1995)
12. Deshpande M R et al. *Phys. Rev. Lett.* **76** 1328 (1996); Sleight J W et al. *Phys. Rev. B* **53** 15727 (1996); *Semicond. Sci. Technol.* **9** 1919 (1994)
13. Schmidt T et al. *Europhys. Lett.* **36** 61 (1996)
14. Sivan U et al. *Europhys. Lett.* **25** 605 (1994)
15. Glazman L I, Matveev K A *Pis'ma Zh. Eksp. Teor. Fiz.* **48** 403 (1988) [*JETP Lett.* **48** 445 (1988)]; Chen L Y, Ting C S *Phys. Rev. B* **44** 5916 (1991)
16. Chaplik A, Èntin M V *Zh. Eksp. Teor. Fiz.* **67** 208 (1974) [*Sov. Phys. JETP* **40** 106 (1974)]; Azbel M Ya *Solid State Commun.* **45** 527 (1983); Xue W, Lee P A *Phys. Rev. B* **38** 3913 (1988)
17. Thouless D J *Phys. Rev. Lett.* **39** 1167 (1977)
18. Fal'ko V I *Phys. Rev. B* **56** 1049 (1997)
19. Al'tshuler B L, Khmel'nitskii D E *Pis'ma Zh. Eksp. Teor. Fiz.* **42** 291 (1985) [*JETP Lett.* **42** 359 (1985)]
20. Xiong S, Stone A D *Phys. Rev. Lett.* **68** 3757 (1992)
21. Geim A K et al. *Phys. Rev. Lett.* **67** 3014 (1991); *Phys. Rev. Lett.* **69** 1248 (1992)
22. Maslov D L, Loss D *Phys. Rev. Lett.* **71** 4222 (1993); Khmel'nitskii D E, Yosefin M *Surf. Sci.* **305** 507 (1994)

Resonant tunneling through a single-electron transistor

J König, H Schoeller, G Schön

1. Introduction

Electron transport through mesoscopic metallic islands and quantum dots is strongly influenced by the large charging energy, $E_C = e^2/2C$, associated with the low capacitance C of the system [1–3]. In the prototype of these systems, the ‘single-electron transistor’, a small island is coupled via tunnel junctions to leads and via a capacitor to a gate voltage source. At low temperatures, $T \ll E_C$, a variety of single-electron phenomena have been observed, including a Coulomb blockade and oscillations of the conductance as a function of the gate voltage.

The detailed features of the transport properties depend on the properties of the island. We consider here two opposite limits. In the first, the island contains a continuum of states, and the tunnel junctions are ‘wide’ with a large number of transverse channels. This is typically realized in metallic grains. If the dimensionless tunneling conductance of the junctions between the island and the lead electrodes,

$$\alpha_t \equiv \frac{R_K}{4\pi^2 R_t} \quad (1)$$

is low, on a scale given by the quantum resistance $R_K = h/e^2 \simeq 25.8 \text{ k}\Omega$, the island charge is well-defined.

In the second limit, we consider the extreme case of an island containing one spin-degenerate level in the interesting energy range. This accounts for Coulomb blockade phenomena in zero-dimensional systems, such as double-barrier resonant-tunneling structures [4, 5], split-gate quantum-dot devices [6–8], quantum point-contacts with single-charge trap states [9], and ultra-small metallic tunnel junctions [10] with particles of diameter below 10 nm. In these islands the discrete level spectrum can be resolved, with a level spacing δ which may exceed T and eV . The coupling between the island and the leads is then characterized by the intrinsic level broadening in the non-interacting case Γ .

For $\alpha_t \ll 1$ in metallic islands or $\Gamma \ll T$ in quantum dots, sequential single-electron tunneling can be studied using perturbation theory [1, 3, 11–15]. On the other hand, recent experiments with strong tunneling show deviations from the classical description. In the metallic case, a broadening of the conductance peaks much larger than temperature has been observed [16, 17], demonstrating the effect of quantum fluctuations and higher-order coherent processes. Several theoretical papers [18–24] dealt with the problem of higher-order processes. This includes ‘inelastic co-tunneling’ [25, 24], where, in a second-order process in α_t , electrons tunnel via a virtual state of the island. (The term ‘inelastic’ indicates that with overwhelming probability different electron states are involved in the different steps of the correlated processes.) An extension of this process, which gains importance near resonances, is ‘inelastic resonant tunneling’ [20, 23], a process where electrons tunnel an arbitrary number of times between the reservoirs and the islands.

The quantum dot is described by the Anderson impurity model where the level is coupled via tunneling barriers to electron reservoirs. A strong on-site Coulomb repulsion suppresses double occupancy of the dot level. From the

theory of strongly correlated fermions [26] it is known that at equilibrium the spectral density of the dot can exhibit a Kondo resonance at the Fermi level, which leads to an increased linear conductance (Kondo-assisted tunneling) [27, 28]. A more pronounced feature has been observed in the nonlinear conductance, which shows a zero-bias maximum even for temperatures above the Kondo temperature [29, 30].

This article is devoted to the calculation of the conductance of a SET transistor beyond sequential tunneling. Since the strong Coulomb interaction between the island electrons cannot be handled in ordinary perturbation theory, we explicitly keep track of the degrees of freedom responsible for the interaction, but eliminate all other degrees of freedom. The resulting reduced density matrix then characterizes the time evolution of the system. In the metallic case the situation is complicated by the fact that the island contains a large number of electrons. In this case a Hubbard–Stratonovich transformation introduces a collective variable replacing the interaction between the electrons. We derive a diagrammatic expansion in which we can identify sequential, co- and resonant tunneling processes with certain classes of diagrams. We present different approximation schemes to evaluate the spectral function and the conductance of the system.

2. Metallic island

We consider a metallic island coupled by two tunnel junctions (L, R) to two leads and capacitively to an external gate voltage V_g . An applied transport voltage $V = V_L - V_R$ drives a current. A microscopic description of this single-electron transistor is based on the Hamiltonian, $H = H_L + H_R + H_I + H_{ch} + H_{t,L} + H_{t,R}$. Here

$$H_r = \sum_{k\sigma} \epsilon_{k\sigma} a_{k\sigma}^\dagger a_{k\sigma}$$

describes non-interacting electrons in the left and right lead, $r = L, R$, and

$$H_I = \sum_{q\sigma} \epsilon_{q\sigma} c_{q\sigma}^\dagger c_{q\sigma}$$

models the island states. The Coulomb interaction is accounted for in a capacitance model

$$H_{ch} = E_C \left(\sum_{q\sigma} c_{q\sigma}^\dagger c_{q\sigma} - n_g \right)^2.$$

The energy scale $E_C \equiv e^2/2C$ of the transistor depends on the total island capacitance, $C = C_L + C_R + C_g$, given by the two tunnel junction and the gate capacitance. The charging energy can be tuned continuously by the ‘gate charge’ $en_g = C_L V_L + C_R V_R + C_g V_g$. The tunneling Hamiltonian

$$H_{t,r} = \sum_{kq\sigma} (T^{\sigma r} a_{k\sigma}^\dagger c_{q\sigma} + \text{H.c.})$$

describes tunneling between the island and the leads. The matrix elements are related to the tunnel conductances by

$$R_r^{-1} = \frac{e^2}{h} \sum_{\sigma} N_r^{\sigma}(0) N_I^{\sigma}(0) |T^{\sigma r}|^2,$$

where $N(0)$ denotes the densities of states of the island and the leads, respectively. We consider ‘wide’ metallic junctions with $N \gg 1$ transverse channels. Extending the spin summation they can be labeled by the index $\sigma = 1, \dots, N$. In the following we will put $\hbar = 1$.

Our aim is to study the time evolution of the reduced density matrix. We shortly sketch the main steps of the derivation of this description.

(1) The time evolution of the density matrix introduces a forward and a backward propagator, which get coupled when we trace out the electron degrees of freedom of the reservoirs. This procedure is known from the work of Caldeira and Leggett [31] who, generalizing earlier work of Feynman and Vernon, studied the influence of Ohmic dissipation on a quantum system. Similarly the influence on electron tunneling for a single tunnel junction was described in Refs [32, 2].

(2) In order to describe the Coulomb interaction between electrons, we introduce via a Hubbard–Stratonovich transformation the electric potential of the island $V(t)$ as a macroscopic field, i.e., the interaction between electrons is replaced by an interaction with the collective variable.

(3) We treat the leads, as well as the electrons, in the island as large equilibrium reservoirs with fixed electrochemical potentials $\mu_r = -eV_r$ for the leads ($r = L, R$). The fluctuating voltage of the island $V(t) \equiv -\dot{\varphi}(t)/e$ is related to a phase $\varphi(t)$. Its quantum mechanical conjugate is the number of excess electrons $n(t)$ on the island. Since it is independent of the microscopic degrees of freedom described by $c_{q\sigma}$ and $c_{q\sigma}^\dagger$, the electronic degrees of freedom can be traced out.

(4) The time evolution of the reduced density matrix $\rho(t; \varphi_1, \varphi_2)$ can thus be expressed by a double path integral over the phases corresponding to the forward and backward propagators φ_j ($j = 1, 2$). We combine the two integrations to a single integral along the Keldysh contour K , which runs from t_i to t_f and back along the real-time axis. The reduced propagator Π is then

$$\Pi = \text{tr} \left[\rho_0 T_K \exp \left(-i \int_K dt H(t) \right) \right] \\ = \int D[\varphi(t)] \exp \left\{ i(S_{ch}[\varphi(t)] + S_t[\varphi(t)]) \right\}. \quad (2)$$

Here the collective variable $\varphi(t)$ and the time integral are defined on the Keldysh contour, and the time-ordering operator T_K orders the following operators accordingly.

The first term of the effective action entering the propagator represents the charging energy

$$S_{ch}[\varphi(t)] = \int_K dt \left\{ \frac{C}{2} \left[\frac{\dot{\varphi}(t)}{e} \right]^2 + n_g \dot{\varphi}(t) \right\}.$$

Electron tunneling is described by $S_t[\varphi(t)]$, which, in the case of wide metallic junctions, is expressed by the simplest electron loop connecting two times,

$$S_t[\varphi(t)] = 2\pi i \sum_{r=L,R} \int_K dt \\ \times \int_K dt' \alpha_r^K(t, t') \exp[i\varphi(t)] \exp[-i\varphi(t')]. \quad (3)$$

The kernels $\alpha_r^K(t, t') = \alpha_r^\pm(t - t')$ for $t < t'$ ($t > t'$) depend on the order of the times along the Keldysh contour.

Their Fourier transforms are [2, 20, 23]

$$\alpha_r^\pm(\omega) = \pm \alpha_{t,r} \frac{\omega - \mu_r}{\exp[\pm(\omega - \mu_r)/T] - 1} \quad (4)$$

with $\alpha_{t,r} = h/(4\pi^2 e^2 R_r)$. In the following we use the notations $\alpha_r(\omega) = \alpha_r^+(\omega) + \alpha_r^-(\omega)$ and $\alpha(\omega) = \sum_r \alpha_r(\omega)$.

To proceed we change from the phase to the charge representation. The time evolution of the density matrix then depends on the propagator from n_1 forward to n'_1 and on the backward branch from n'_2 backward to n_2 with matrix elements [23]

$$\begin{aligned} \Pi_{n_2, n'_2}^{n_1, n'_1} &= \int d\varphi_1 \int d\varphi'_1 \int d\varphi'_2 \int d\varphi_2 \\ &\times \int_{\varphi_2, \varphi'_2}^{\varphi_1, \varphi'_1} D[\varphi(t)] \int D[n(t)] \exp(in_1 \varphi_1) \exp(-in'_1 \varphi'_1) \\ &\times \exp(in'_2 \varphi'_2) \exp(-in_2 \varphi_2) \\ &\times \exp\left(-iS_{\text{ch}}[n(t)] + iS_t[\varphi(t)] + i \int_K dt n(t) \dot{\varphi}(t)\right), \end{aligned} \quad (5)$$

in which $S_{\text{ch}}[n(t)] = \int_K dt E_C [n(t) - n_g]^2$.

3. Expansion in the tunneling conductance

To obtain a diagrammatic description we expand the tunneling term $\exp(iS_t[\varphi(t)])$ in Eqn (5). Each of the exponentials $\exp[\pm i\varphi(t)]$ describes the tunneling of an electron at time t . These changes occur in pairs in each junction, $r = L, R$, and are connected by tunneling lines $\alpha_r^K(t, t')$. Each term of the expansion can be visualized by a diagram. Several examples are displayed in Fig. 1. The diagram is calculated according to rules which follow from the expansion of Eqn (5), (for details see Ref. [23]).

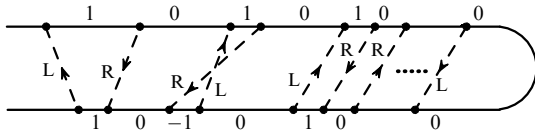


Figure 1. From left to right: sequential tunneling in the left and right junction, a co-tunneling process, and resonant tunneling.

The propagator from a diagonal state n to another diagonal state n' is denoted by $\Pi_{n,n'}$. It is the sum of all diagrams with the given states at the ends and can be expressed by an irreducible self-energy part $\Sigma_{n,n'}$, defined as the sum of all diagrams in which any vertical line cutting through them crosses at least one tunneling line. The propagator can be expressed as an iteration in the style of a Dyson equation,

$$\Pi_{n,n'} = \Pi_n^{(0)} \delta_{n,n'} + \sum_{n''} \Pi_{n,n''} \Sigma_{n'',n'} \Pi_{n'}^{(0)}.$$

The term $\Pi^{(0)}$ describes a propagation which does not contain a tunneling line. The probability for state n follows from

$$P_n = \sum_{n'} P_{n'}^{(0)} \Pi_{n',n}$$

(with $P_n^{(0)}$ being the initial distribution). Our diagram rules yield

$$\frac{d}{dt} P_n = -i \sum_{n' \neq n} [P_n \Sigma_{n,n'} - P_{n'} \Sigma_{n',n}]. \quad (6)$$

We recover the structure of a master equation with transition rates given by $\Sigma_{n',n}$. In general, the irreducible self-energy Σ yields the rate of all possible correlated tunneling processes. We reproduce the well-known single-electron tunneling rates by evaluating all diagrams which contain no overlapping tunneling lines. Similarly co-tunneling is described by the diagrams where two tunneling lines overlapping in time, as shown in Fig. 1.

We calculate the current I_r flowing into reservoir $r = L, R$ by adding a source term to the Hamiltonian and then taking the functional derivative of the reduced propagator with respect to the source. The result

$$I_r = -ie \int d\omega \{ \alpha_r^+(\omega) C^>(\omega) + \alpha_r^-(\omega) C^<(\omega) \}$$

is expressed by the correlation functions

$$\begin{aligned} C^>(t, t') &= -i \langle \exp[-i\varphi(t)] \exp[i\varphi(t')] \rangle, \\ C^<(t, t') &= i \langle \exp[i\varphi(t')] \exp[-i\varphi(t)] \rangle. \end{aligned}$$

These are related to the spectral density by $2\pi i A(\omega) = C^<(\omega) - C^>(\omega)$.

For sequential tunneling, the current reduces to

$$I_r = \frac{4\pi^2 e}{h} \int d\omega \sum_{r'} \frac{\alpha_{r'}(\omega) \alpha_r(\omega)}{\alpha(\omega)} A(\omega) [f_{r'}(\omega) - f_r(\omega)], \quad (7)$$

with

$$A^{(0)}(\omega) = \sum_{n=-\infty}^{\infty} [P_n + P_{n+1}] \delta(\omega - \Delta_n)$$

and $\Delta_n = E_{\text{ch}}(n+1) - E_{\text{ch}}(n) = E_C [1 + 2(n - n_g)]$, where the probabilities follow from $P_n \alpha^+(\Delta_n) - P_{n+1} \alpha^-(\Delta_n) = 0$.

To go beyond we have to choose a systematic criterion by which higher-order contributions should be included. One possibility is to take into account all second-order terms (co-tunneling). At the minima of the Coulomb oscillations the system is in the Coulomb blockade regime, and co-tunneling processes dominate the conductance. A careful analysis of our diagrammatic expansion not only reproduces the known limits [25] but also provides the needed regularization of divergences. We, furthermore, obtain new terms describing the renormalization of the system parameters, which is essential at the resonance. These results are presented in Ref. [24].

The stronger the quantum fluctuations are, either because α_t is large or the temperature is low, the more important are contributions of higher order. We can sum them, in a conserving approximation, as long as we restrict ourselves to matrix elements of the density matrix which are at most two-fold off-diagonal [23]. If we further consider only two adjacent charge states, $n = 0, 1$, which is reasonable when the energy difference of the two states Δ_0 , the bias voltage $eV = eV_L - eV_R$, and the temperature T are low compared to E_C , we can evaluate the irreducible self-energy analytically. The following results are derived for this limit.

We find that the current is given by Eqn (7), but with the spectral density

$$A(\omega) = \frac{\alpha(\omega)}{[\omega - \Delta_0 - \text{Re } \sigma(\omega)]^2 + [\text{Im } \sigma(\omega)]^2}. \quad (8)$$

A complex self-energy $\sigma(\omega)$ accounts for energy renormalization and life-time broadening effects via

$$\begin{aligned} \text{Re } \sigma(\omega) &= -2 \sum_r \alpha_{t,r}(\omega - \mu_r) \\ &\times \left[\ln \left(\frac{E_C}{2\pi T} \right) - \text{Re } \Psi \left(\frac{i(\omega - \mu_r)}{2\pi T} \right) \right], \\ \text{Im } \sigma(\omega) &= -\pi \alpha(\omega). \end{aligned}$$

The quantum fluctuations have a pronounced influence on the differential conductance $G = \partial I / \partial V$. In Figure 2 we present our results for the maximal differential conductance in the linear response regime ($V = 0$). The asymptotic high-temperature conductance is $G_{\text{as}} = 1/(R_L + R_R)$. At low temperatures, when only two adjacent charge states get occupied, the maximal conductance due to sequential (lowest order) tunneling saturates at one half of the high-temperature value (dashed line 1). The situation changes when higher-order processes are taken into account. For the resonant tunneling approximation (long-dashed line 2) we find that the maximal conductance is renormalized by a factor Z which depends logarithmically on the temperature,

$$Z = \left\{ 1 + 2\alpha_t \ln \left[\frac{E_C}{\max\{eV/2, 2\pi T\}} \right] \right\}^{-1}, \quad (9)$$

i.e. the height of the conductance peak decreases with lower temperatures.

Furthermore, we present the result for co-tunneling (solid line), i.e., for processes up to α_t^2 but including all relevant charge states, thus covering the whole temperature range. Already on this level we find the logarithmic behaviour indicating the renormalization of the conductance. In the experiments of Ref. [16] the conductance α_t is not too large and the co-tunneling theory is sufficient. The good agreement is demonstrated in Fig. 2.

4. Quantum dot

The diagrammatic technique can also be applied to quantum dots [33]. We concentrate here on the limiting case of a single level. The level is either spin degenerate or may be split by a

magnetic field. The Hamiltonian introduced above reduces in this case to the Anderson model $H = H_L + H_R + H_D + H_{t,L} + H_{t,R}$ with

$$H_D = \sum_{\sigma} \epsilon_{\sigma} c_{\sigma}^{\dagger} c_{\sigma} + E_C n_{\uparrow} n_{\downarrow}.$$

The tunnel part reads

$$H_{t,r} = \sum_{k\sigma} (T^{\sigma r} a_{k\sigma}^{\dagger} c_{\sigma} + \text{H.c.}).$$

The tunneling rates in and out of the dot to the reservoir r are in lowest-order perturbation theory in Fourier space

$$\gamma_r^{\pm}(\omega) = \frac{1}{2\pi} \Gamma_r(\omega) f^{\pm}(\omega - \mu_r),$$

with

$$\Gamma_r(\omega) = 2\pi \sum_k |T^{\sigma r}|^2 \delta(\omega - \epsilon_{k\sigma}),$$

$$f^+(\omega) = f(\omega), \quad f^-(\omega) = 1 - f(\omega).$$

The interaction in the system is described by a few degrees of freedom, while we can trace out the reservoirs directly using Wick's theorem. We thus obtain the reduced density matrix which explicitly keeps track of the dot state only. The expansion in the tunneling part leads, then, to a similar diagrammatic representation as in the metallic case. The main difference is, that the tunneling lines [representing the rates $\gamma_R^{\pm}(\omega)$] and the dot states now carry the information of the electron spin.

In order to describe Kondo-like behaviour in quantum dots it is essential to proceed beyond a finite-order perturbation theory. It is reasonable to use the same conserving approximation as for the metallic case, i.e., to take into account non-diagonal matrix elements of the total density matrix up to the difference of one electron-hole pair excitation in the reservoirs. A further motivation of this procedure is the fact that for a system with spinless electrons ($N = 1$) this scheme is exact, since the neglected part adds up to zero.

The current is expressed by the spectral density $A_{\sigma}(\omega)$,

$$I_r = \frac{2\pi e}{h} \int d\omega \sum_{\sigma, \sigma'} \frac{\gamma_{r'}^{\sigma}(\omega) \gamma_r^{\sigma}(\omega)}{\gamma(\omega)} A_{\sigma}(\omega) [f_{r'}(\omega) - f_r(\omega)]. \quad (10)$$

The corresponding correlation functions $C_{\sigma}^{>}(t, t') = -i \langle c_{\sigma}(t) c_{\sigma}^{\dagger}(t') \rangle$ and $C_{\sigma}^{<}(t, t') = i \langle c_{\sigma}^{\dagger}(t') c_{\sigma}(t) \rangle$ are mainly determined by the resolvent $[\omega - \epsilon_{\sigma} - \sigma^{\sigma}(\omega)]^{-1}$ with

$$\begin{aligned} \text{Re } \sigma^{\sigma}(\omega) &= \sum_R \frac{\Gamma_r}{2\pi} \sum_{\sigma' \neq \sigma} \left[\ln \left(\frac{E_C}{2} \right) \right. \\ &\quad \left. - \text{Re } \Psi \left(\frac{1}{2} + \frac{i(\omega + \epsilon_{\sigma'} - \epsilon_{\sigma} - \mu_R)}{2\pi T} \right) \right], \\ \text{Im } \sigma^{\sigma}(\omega) &= -\pi \left[\gamma^{-}(\omega) + \sum_{\sigma'} \gamma^{+}(\omega + \epsilon_{\sigma'} - \epsilon_{\sigma}) \right]. \end{aligned}$$

At zero magnetic field, i.e. $\epsilon_{\sigma} = \epsilon_{\sigma'}$, we can perform the resummation analytically and find

$$A(\omega) = \frac{\gamma^{+}(\omega) + \gamma^{-}(\omega)}{[\omega - \epsilon - \text{Re } \sigma(\omega)]^2 + [\text{Im } \sigma(\omega)]^2}. \quad (11)$$

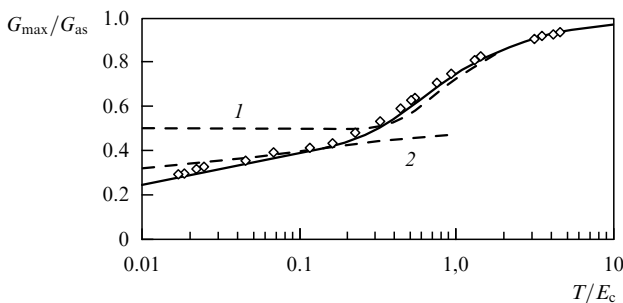


Figure 2. Linear differential conductance normalized to the high temperature limit for sequential tunneling (dashed line 1), sequential plus co-tunneling (solid line) and resonant tunneling (long-dashed line 2) for $\alpha_t = 0.063$. The data points are experimental results from Ref. [16].

In addition to the renormalized level, at low temperature new resonances, the Kondo resonances, emerge near the Fermi levels of the reservoirs. This is due to the logarithmic divergence of $\text{Re } \sigma(\omega)$.

The resonances in the spectral density have pronounced effects on the nonlinear differential conductance as a function of the bias voltage V , as shown in Fig. 3 for the case $\epsilon < 0$. We recover the zero-bias maximum [30, 34] observed in the experiments of Ref. [9]. It arises since the splitting of the Kondo peak with increasing voltage leads to an overall decrease of the spectral density in the energy range $|\omega| < eV$ (see inset of Fig. 3).

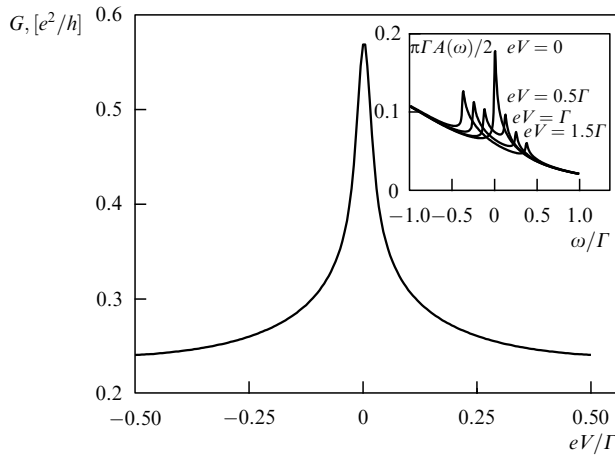


Figure 3. Differential conductance vs. bias voltage for $T = 0.005\Gamma$, $\epsilon = -2\Gamma$, and $E_C = 50\Gamma$. The curves show a maximum at zero bias. Inset: increasing voltage leads to an overall decrease of the spectral density in the range $|E| < eV$.

An applied magnetic field leads to a finite Zeeman energy and lifts the spin-degeneracy. In this case, we have determined the spectral densities numerically. The influence of the self-energy $\sigma^\sigma(\omega)$ on the spectral density $A_\sigma(\omega)$ leads to Kondo resonances at energies $\omega = \mu_r + \epsilon_\sigma - \epsilon_{\sigma'}$ with $\sigma' \neq \sigma$. From Eqn (10) we see that there is no Kondo-assisted tunneling at low transport voltage, but it sets in if the transport voltage and level splitting are equal. Therefore, for low lying levels the conductance peak at zero bias, described in the previous section, now splits into two peaks separated by the twice the level splitting [30] (Fig. 4).

For further extensions, including the effect of double occupancy of the dot level, the influence of a fluctuating environment, as well as tunneling through double-dot systems we refer to Refs [33, 35].

5. Conclusions

We have described single-electron tunneling in systems with strong charging effects beyond perturbation theory in the tunneling conductance. For this purpose we considered the real-time evolution of the reduced density matrix of the system. A systematic diagrammatic expansion allowed us to identify different contributions to the current. When we restrict ourselves to diagrams corresponding to maximally two-fold off-diagonal matrix elements of the density matrix we can formulate a self-consistent resummation of diagrams. At low temperatures the restriction to two adjacent charge states enables us to evaluate the summation in closed form. The most important results are the renormalization of system

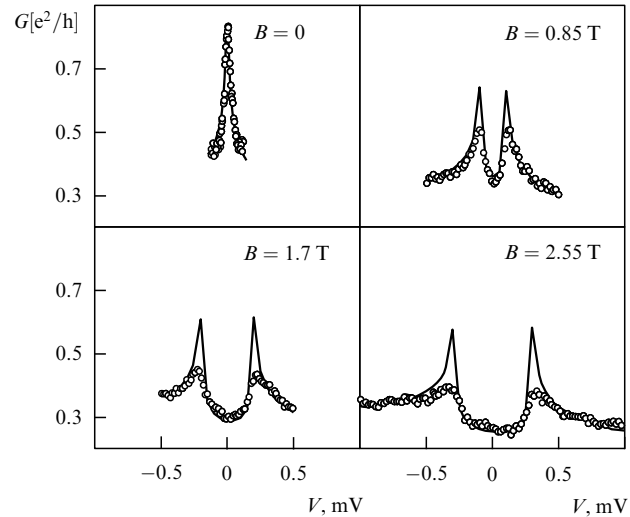


Figure 4. Differential conductance vs. bias voltage for $T = 4.3 \mu\text{eV}$, $\epsilon_\sigma(B=0) = -5.2 \text{ meV}$, $\Gamma = 3.4 \text{ meV}$, $a_C = (C_L - C_R)/C = 0.33$, and $E_C = 30 \text{ meV}$. The circles are data from Ref. [9].

parameters and the life-time broadening of the conductance peaks for the metallic island, as well as Kondo-like behaviour in the quantum dot.

References

- Averin D V, Likharev K K, in *Mesoscopic Phenomena in Solids* (Modern Problems in Condensed Matter Sciences Vol. 30, Eds B L Altshuler, P A Lee, R A Webb) (Amsterdam: North-Holland, 1991) p. 173
- Schön G, Zaikin A D *Phys. Rep.* **198** 237 (1990)
- Single Charge Tunneling: Coulomb Blockade Phenomena in Nanostructures* (NATO ASI Series B, Vol. 294, Eds H Grabert, M H Devoret) (New York: Plenum Press, 1992)
- Su B, Goldman V J, Cunningham J E *Science* **255** 313 (1992)
- Gueret P et al. *Phys. Rev. Lett.* **68** 1896 (1992)
- Johnson A T et al. *Phys. Rev. Lett.* **69** 1592 (1992)
- Foxman E B et al. *Phys. Rev. B* **47** 10020 (1993)
- Weis J et al. *Phys. Rev. B* **46** 12837 (1992)
- Ralph D C, Buhrman R A *Phys. Rev. Lett.* **72** 3401 (1994)
- Ralph D C, Black C T, Tinkham M *Phys. Rev. Lett.* **74** 3241 (1995)
- Averin D V, Korotkov A N, Likharev K K *Phys. Rev. B* **44** 6199 (1991)
- Beenakker C W J *Phys. Rev. B* **44** 1646 (1991)
- Weinmann D et al. *Europhys. Lett.* **26** 467 (1994)
- Bruder C, Schoeller H *Phys. Rev. Lett.* **72** 1076 (1994)
- Glazman L I, Matveev K A *Pis'ma Zh. Eksp. Teor. Fiz.* **48** 403 (1988) [*JETP Lett.* **48** 445 (1988)]
- Joyez P et al. *Phys. Rev. Lett.* **79** 1349 (1997)
- Chouvaev D et al., in preparation
- Matveev K A *Zh. Eksp. Teor. Fiz.* **99** 1598 (1991) [*Sov. Phys. JETP* **72** 892 (1991)]
- Golubev D S, Zaikin A D *Phys. Rev. B* **50** 8736 (1994)
- Schoeller H, Schön G *Phys. Rev. B* **50** 18436 (1994)
- Grabert H *Phys. Rev. B* **50** 17364 (1994)
- Falci G, Schön G, Zimanyi G T *Phys. Rev. Lett.* **74** 3257 (1995)
- König J, Schoeller H, Schön G *Europhys. Lett.* **31** 31 (1995); König J et al., in *Quantum Dynamics of Submicron Structures* (NATO ASI Series E, Vol. 291, Eds H A Cerdeira, B Kramer, G Schon) (Dordrecht, Boston: Kluwer Academic, 1995) p. 221
- König J, Schoeller H, Schön G *Phys. Rev. Lett.* **78** 4482 (1997)
- Averin D V, Nazarov Yu V, in Ref. [3]
- Bickers N E *Rev. Mod. Phys.* **59** 845 (1987)
- Ng T K, Lee P A *Phys. Rev. Lett.* **61** 1768 (1988)
- Glazman L I, Raikh M E *Pis'ma Zh. Eksp. Teor. Fiz.* **47** 378 (1988) [*JETP Lett.* **47** 452 (1988)]

29. Hershfield S, Davies J H, Wilkins J W *Phys. Rev. Lett.* **67** 3720 (1991); *Phys. Rev. B* **46** 7046 (1992)
30. Meir Y, Wingreen N S, Lee P A *Phys. Rev. Lett.* **70** 2601 (1993); Wingreen N S, Meir Y *Phys. Rev. B* **49** 11040 (1994)
31. Caldeira A O, Leggett A J *Ann. Phys. (N.Y.)* **149** 374 (1983)
32. Eckern U, Schön G, Ambegaokar V *Phys. Rev. B* **30** 6419 (1984)
33. König J, Schoeller H, Schön G *Phys. Rev. Lett.* **76** 1715 (1996); König J et al. *Phys. Rev. B* **54** 16820 (1996)
34. Hettler M H, Schoeller H *Phys. Rev. Lett.* **74** 4907 (1995)
35. Pohjola T et al. submitted to *Europhys. Lett.*

Coulomb-like mesoscopic conductance fluctuations in a 2D electron gas near the filling factor $\nu = 1/2$

Z D Kvon, E B Olshanetskiĭ, G M Gusev,
J C Portal, D K Maude

More than a decade after its discovery, the fractional quantum Hall effect (FQHE) still remains in the focus of attention in solid state physics. Recently a new approach to the FQHE, the composite fermion theory, has been proposed [1, 2]. According to this approach strongly interacting 2D electrons at a fractional filling of the first Landau level can be viewed as a gas of novel weakly interacting quasiparticles, the so called composite fermions (CF), that have a renormalized effective mass and are expected to exhibit a number of semiclassical properties. The FQHE for electrons is then explained as an IQHE for CF moving in an effective magnetic field $B_{\text{eff}} = B - B_{1/2}$, where B is the applied magnetic field and $B_{1/2}$ — the magnetic field corresponding to the half filling of the first Landau level. It is noteworthy that all the main predictions of the CF theory have been shown to be basically true in numerous and diverse experiments [3–10]. The described approach to the FQHE raises a number of questions concerning quantum interference and, in particular, the nature and properties of universal conductance fluctuations (UCF) at a fractional Landau level filling. Recently a theory has been proposed [11] which deals with UCF in the presence of a random magnetic field. The results of this theory have been used to describe the behaviour of a gas of CF in a system with random potential fluctuations. The authors of Ref. [11] come to the conclusion that in the case of CF the Fermi energy dependence of UCF is radically different from that of electrons at $B = 0$. The gate voltage dependence of CF conductance fluctuations at $\nu = 1/2$ is predicted to be similar in some respect to aperiodical Coulomb-like oscillations with an effective charge $e/2$.

It appears that the first observation of conductance fluctuations in magnetoresistance dependencies in the vicinity of $\nu = 1/2$ was made in a ballistic microbridge in Ref. [12]. However the absence of any analysis of these fluctuations in Ref. [12] makes it difficult to completely exclude the possibility of these fluctuations being some kind of noise. A more detailed experimental study of the magnetoresistance conductance fluctuations in the vicinity of $\nu = 1/2$ was reported recently in Ref. [13]. The authors performed a comparison analysis of these fluctuations and of the UCF around $B = 0$ and came to the conclusion that the fluctuations observed at $\nu = 1/2$ could indeed be described as UCF of CF. The latter experiment, however, was limited to the study of magnetoresistance dependences and lacked measure-

ments of CF conductance versus Fermi energy necessary for testing the important theoretical prediction mentioned above [11].

In the present work we have investigated the behaviour of mesoscopic samples in the vicinity of the half filling of the first Landau level. Both the magnetic field and gate voltage dependencies of mesoscopic fluctuations near $\nu = 1/2$ were studied. It was found that in contrast to the case of mesoscopic fluctuations in weak magnetic fields, in the vicinity of $\nu = 1/2$ there exists a special relation between the R_{xx} fluctuations in the resistance versus magnetic field and in the resistance versus gate voltage dependencies. Namely the ratio of the correlation magnetic field to the correlation electron density is found to be equal with fairly good precision to $2\Phi_0$ (where Φ_0 is the magnetic flux quantum) i.e. to be determined solely by the Landau level filling factor. In our opinion this experimental evidence corroborates the prediction of Ref. [11] and mesoscopic conductance fluctuations in the vicinity of $\nu = 1/2$ can indeed be viewed as Coulomb-like aperiodical fluctuations with a corresponding effective charge $e/2$.

Our two experimental samples were microbridges with lithographical length $L = 2 \mu\text{m}$ and width $W = 1 \mu\text{m}$. The actual width of the microbridges determined from Shubnikov–de Haas oscillations in weak magnetic fields is $(0.3–0.5) \mu\text{m}$. The microbridges were fabricated by means of electron lithography and plasma chemical etching on top of a 2D electron gas in an AlGaAs/GaAs heterolayer with a spacer thickness of 60 nm. The electron density and electron mobility in the original heterolayers were $(1–2) \times 10^{11} \text{ cm}^{-2}$ and $(2–4) \times 10^5 \text{ cm}^2 (\text{V} \cdot \text{s})^{-1}$ respectively. The microbridges were etched in the middle between the voltage probes of a conventional rectangular Hall bar with dimensions $100 \times 50 \mu\text{m}^2$. At the final stage of preparation the structures were covered by an Au/Ni metal gate. The schematic top view of the structures is shown in the inset to Fig. 1. The measurements were carried out at temperatures of 30 mK – 4.2 K in magnetic fields up to 15 T. The alternating driving current of frequency 3–6 Hz was kept as low as $(0.5–1) \text{ nA}$ to preclude electron heating.

Figure 1 shows a typical $R_{xx}(B)$ curve for sample I at a gate voltage of +350 mV. One can see distinct minima corresponding to $\nu = 1$ and $\nu = 2$ and a weaker minimum at $B = 8.5 \text{ T}$ corresponding to $\nu = 2/3$ in the microbridge. The fact that R_{xx} does not become zero at $\nu = 1$ and $\nu = 2$ testifies

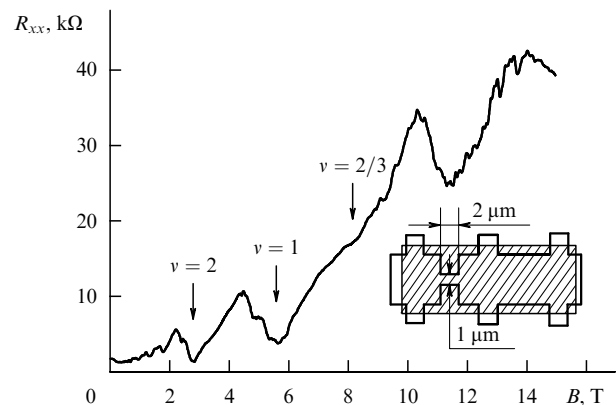


Figure 1. Sample I, $R_{xx}(B)$; $T = 30 \text{ mK}$, $V_g = 350 \text{ mV}$. Inset: schematic top view of the experimental samples; the region under gate is hatched.